Skeletal Surrogate Metastructural Anisotropy Mimicry and the Influence of Fabrication Material

B. S. Hezrony[1], P. C. F. Lopes[2], and P. J. Brown[1]
[1] Wake Forest University/Virginia Tech School of Biomedical Engineering and Sciences, US
[2] Universidade Federal Fluminense – Insituto de Computação, BR

ABSTRACT

Human Body Models have been used for decades to inform efforts in promoting automobile occupant and pedestrian safety. However, many of these models fail to capture the intricacies of individual variability. Cadaveric subjects typically exceed representative age ranges and hence mechanics. Animal subjects typically require specific setups that stray from that which is representative of human crash scenarios. Computational models can only consider so many practical real-world variables. Artificial surrogates, dummies being popular among them, are very popular for reusability and robust data collection. However, even the biomechanically accurate skeletal surrogates available commercially are limited in that they do not consider human variability and skeletal microstructure local variability. The objective of the work herein is to assess computational methods of metastructural variability mimicry by fabrication material. We implement mimicry approaches focusing on bulk isotropic elasticity, and in-house structural optimization approaches focusing on pure anisotropy skeletal microstructure mimicry. This allows us to assess rapid and detailed approaches alike and determine which fabrication materials are ideal under which approach. We found that Fortify DT was ideal for mimicking the phenomena present in the GHBMC M50 L5 model when using a walled Gyroid. For microstructural mimicry, we found there to be a range in acceptable bulk material elastic moduli between 2.98 and 36.6 GPa. Ultimately, these findings have the potential to guide practitioners of skeletal microstructure biomimicry.

INTRODUCTION

Since the 1979 introduction of National Highway Traffic Safety Administration (NHTSA) crash testing, the automotive accident-related death rate per 100 million miles driven in the US between 1979 and 2022 has declined by about 66% (National Safety Council, 2023). NHTSA crash testing involves rigorous experimentation to ensure that automobiles achieve set safety standards, with a goal being the minimization of human risk. A major innovation in car crash testing is the incorporation of the Human Body Model (HBM). HBMs are crucial in several modern engineering disciplines not limited to biomedical, automotive, mechanical, aerospace, etc. Physically, they encompass cadaveric models, animal models, crash dummies, and even manufactured hard and soft tissue surrogates.

This paper is a student paper from the 19th Injury Biomechanics Symposium and is published in a special issue of SAE International Journal of Transportation Safety.
It is preliminary work, has not been peer reviewed, and should not be cited because it is a work in progress.

Despite the development and commercial success of biomechanical skeletal surrogates, demographically diverse representation of the skeletal microstructure and inherent spatially variate isotropic and anisotropic elasticity in HBMs has been amiss. With an abundance of disease states and *in vivo* variability, the introduction of microstructural variability mimicry into manufactured surrogates may be the next horizon. To further Diversity, Equity, and Inclusion (DEI) in automotive standards assessment, such multivariate features may one day be desirable. The work herein serves to identify the materials, via computational analysis, that would inform such experimental efforts. It is hypothesized that inverse design approach success is primarily dependent on the materials modeled.

METHODS

Two vastly different approaches for inverse design are implemented herein. The first method is that of spatially variate isotropic elasticity variability via a field-based power law relationship. This approach is the most efficient, robust, and easy to implement. However, it only makes use of clinical resolution information. The second approach is that of bottom-up purely anisotropic inverse homogenization. Relatively, it is an inefficient, computationally demanding, and maximally involved in implementation. Here, isotropic mimicry is performed on a whole vertebral body in multiple materials, while anisotropic mimicry is performed on small cubic specimens from cadaveric femoral High-Resolution peripheral Quantitative Computed Tomography (HR-pQCT) data in multiple mimicry materials. Because the approaches are vastly different, the results are limited in comparability. However, both provide unique insight into the current state of computational methods for skeletal structure mimicry.

Isotropic Mimicry Approach

To develop an organic method for producing structures that mimic microstructural properties, the following approach was taken. It has been shown that for porous, smooth structures, the following relates unit cell-based volume fraction to elastic modulus (Gibson et al., 1982; Gibson & Ashby, 2014; Refai et al., 2020):

$$E_{Bulk}/E_{Cell} = C_1\left(V_{Bulk}/V_{Cell}\right)^m \rightarrow \bar{\rho} = \sqrt[m]{\frac{1}{C_1}\frac{E_{Bulk}}{E_{Cell}}} \qquad [1]$$

where V_{Bulk} is the volume of bulk material in the cell, V_{Cell} is the volume of the cell, $\bar{\rho}$ is the unit cell volume fraction, E_{Cell} is the unit cell equivalent elastic modulus, E_{Bulk} is the bulk elastic modulus of the material, and C_1 and m are empirical constants for the walled Gyroid. The walled Gyroid field equation, $F(x, y, z)$, and field parameter, t, are defined as such:

$$t = 3(\bar{\rho} - 0.5) \qquad [2]$$

$$F(x,y,z) = \left(sin\left(\frac{2\pi x}{L}\right)cos\left(\frac{2\pi y}{L}\right) + sin\left(\frac{2\pi y}{L}\right)cos\left(\frac{2\pi z}{L}\right) + sin\left(\frac{2\pi z}{L}\right)cos\left(\frac{2\pi x}{L}\right)\right)^2 = t^2 \qquad [3]$$

where t is the parameterization variable, x, y, and z are coordinates, and L is the length of a unit cell. [2] relates t to $\bar{\rho}$ (Scherer, 2013). Rearranging, an implicit Gyroid geometry, $I(x, y, z)$, is defined that matches elasticity for structures, in an isotropic material with E_{Bulk}:

This paper is a student paper from the 19th Injury Biomechanics Symposium and is published in a special issue of SAE International Journal of Transportation Safety.
It is preliminary work, has not been peer reviewed, and should not be cited because it is a work in progress.

$$I(x,y,z) = F(x,y,z) - \left(3\left(\sqrt[m]{\frac{1}{C_1}\frac{E_{Bulk}}{E_{Cell}}} - 0.5\right)\right)^2 = 0 \quad [4]$$

Five materials common in biomedical AM are tested in simulation by applying reported material properties (Table 1, presented in the Results section) to the finite element (FE) models. The above defined implicit topology is modeled using a FE shell mesh. Because the same mesh, which models the implicit mid-plane, could represent any such topology independent of local thickness, the same shell mesh is used across multiple material simulations. Limiting computational cost, the only variables changed are elasticity and the corresponding mesh thickness. This keeps effective microstructural elasticity constant. The required volume fraction, and thus the required structural thickness, is calculated based on the desired elastic modulus of the trabecular structure, a constant among all simulations based on the ground truth Global HBM Consortium (GHBMC) male 50th percentile (M50) L5 model assuming linear behavior (0.38 GPa). The desired volume fraction of the Gyroid structure is calculated using equations from Gibson et. al. (Gibson et al., 1982; Gibson & Ashby, 2014), relating the volume fraction of a fine cell-based structure to its properties relative to the bulk material. From this, the desired structural thickness is calculated using an empirically derived relationship between Gyroid volume fraction and thickness from MATLAB and nTop, the software used to create the initial shell mesh and perform topological calculations. The result is the Gyroid shell model depicted in Figure 1A for a high rigidity material and Figure 1B for a low rigidity material. Cortical faces are tied to trabecular nodes with a 0.1 mm tolerance. A pressure is applied to the superior cortical mesh, reflecting loading at rest and in an automotive accident in a 50th percentile male. L5 loading was simulated in sitting conditions, and in crash conditions based on: (1) the loads acting on lumbar spine when seated: $F_{L4L5,sitting} \approx 84.94$ N; (2) the biomechanics of lumbar segments in compression: $F_{L4L5,accident} \approx 10.94$ kN (130x seated), at 2.24 MPH. Implicit and modal simulations were performed for both states. Figure 2 shows the GHBMC L5, with the superior cortical elements loaded normally and the inferior nodes being fixed. The same procedure for node tying is used for the solid element GHBMC model and the shell element Gyroid model.

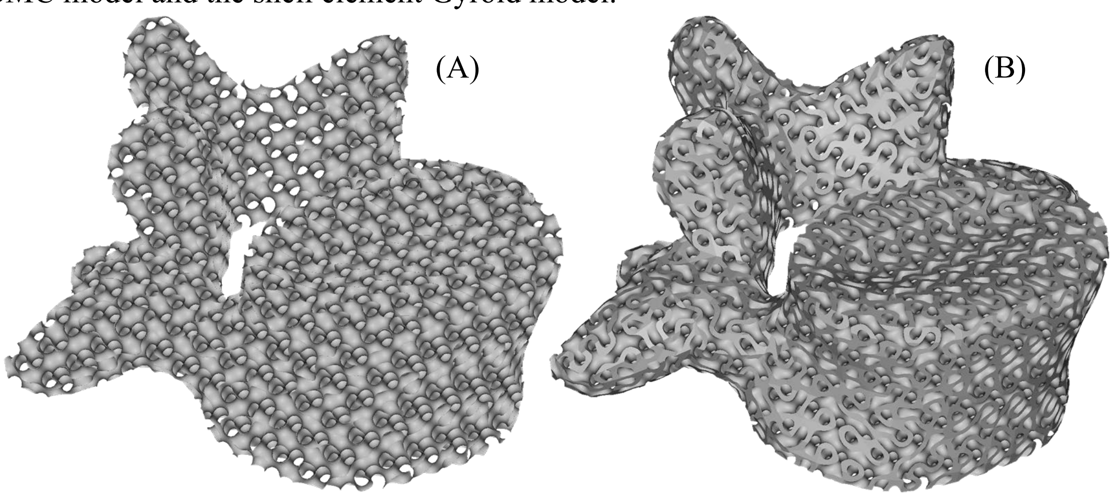

Figure 1: Influence of material variation on geometry of a unit-cell-stiffness-matched L5 surrogate (A) in relatively high rigidity Ti-6Al-4V (116 GPa) yielding a thinner structure than (B) CE 221 (3.9 GPa).

This paper is a student paper from the 19th Injury Biomechanics Symposium and is published in a special issue of SAE International Journal of Transportation Safety.
It is preliminary work, has not been peer reviewed, and should not be cited because it is a work in progress.

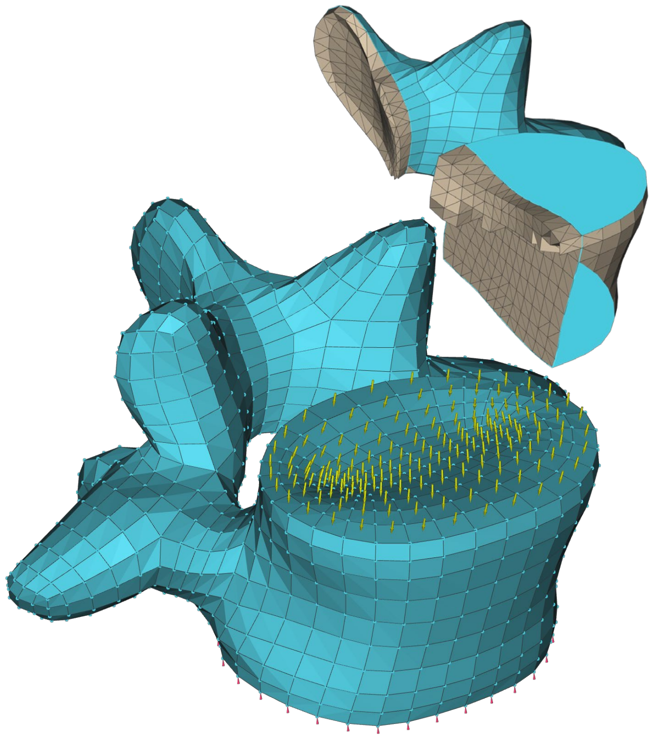

Figure 2: GHBMC L5 model cross-section and distributed load.

Anisotropic Mimicry Approach

A level-set algorithm for topological shape optimization is developed, and the classic inverse homogenization (IH) theory of strain energy volumetric averaging is followed (Sigmund, 1994). Algorithms inspired by Lopes et al., 2022, are implemented to accelerate forward analysis (Lopes et al., 2022). To validate efficacy on skeletal inverse homogenization, 24 cadaveric HR-pQCT proximal femur scans are considered from publicly available data (Hazrati-Marangalou et al., 2013). Central 4 mm side length samples are selected by volume fraction from the femoral head, neck superior, neck inferior, trochanter superior, trochanter middle, and trochanter inferior. As such, there are 144 unique cubic specimens. Twenty materials are assessed for each of these specimens, resulting in 2,880 inverse homogenizations. Constraint satisfaction and duration of inverse homogenization are the metrics of interest. It is anticipates that the foremost determinant of constraint satisfaction is material selection rather than anatomic region, and that duration of inverse homogenization follows a similar trend.

Statistical Approach. Constraint satisfaction is a binary outcome and duration is a continuous outcome. Material is stratified continuously via Elastic Modulus. Anatomic region is stratified as a categorical variable. At each material and/or region, the data spread is assessed. Constraint satisfaction is modeled using a set of binomial distributions, while duration is modeled

This paper is a student paper from the 19th Injury Biomechanics Symposium and is published in a special issue of SAE International Journal of Transportation Safety.
It is preliminary work, has not been peer reviewed, and should not be cited because it is a work in progress.

using a set of Gaussian distributions. Statistically insightful characteristic curves for constraint satisfaction and IH duration with varying material elasticity is an outcome of interest.

RESULTS

Isotropic Mimicry Results

In the GHBMC M50 model, the trabecular region has a 0.38 GPa elastic modulus, and the cortical region has an 18.44 GPa elastic modulus. The properties of the printable materials are shown in Table 1 and in Figure 3, including elastic modulus, elongation at break, and ultimate strength. 95^{th} percentile maximum strain, 95^{th} percentile maximum Von Mises Stress (VMS), and failure outcomes relative to max elongation and/or maximum strength are reported for the static analyses. For the modal analyses, minimum buckling load factor and presence of buckling failure are reported. In both the accident and seated scenarios, Fortify DT has 95^{th} percentile max principal strain and VMS most like that in the GHBMC model. In terms of VMS, the response has % difference (PD) of 1.38% (seated) and 0.62% (accident). Otherwise, average PD is about 80% for the other materials. In modal response, average PD is over 140% for the other materials, again with the GHBMC as the baseline and PD being computed per material/condition. The buckling load factor PD in an accident scenario with Fortify DT is 17.7%, with PD in the seated scenario being on par with the average material PD.

Table 1: Results of FEA

	Input			Output						
Material:	Youngs' Modulus (GPa):	Elongation at Break (%):	Ultimate Strength (MPa):	Condition:	Thickness (mm):	95th Percentile Max Principal Strain (%):	95th Percentile Von-Mises Stress (MPa):	Failure in Compression?	Min. Buckling Load Factor:	Failure in Buckling?
Ti-6Al-4V	116	10	1000	Sitting	0.0458	0.01	12.90	NO	18.640	NO
				Accident		1.60	1662.17	YES	0.302	YES
Fortify DT	7.35	1.8	90	Sitting	0.5146	0.01	0.72	NO	2108.934	NO
				Accident		1.43	92.82	YES	16.375	NO
CE 221	3.9	3	85	Sitting	0.8972	0.01	0.39	NO	3508.044	NO
				Accident		1.45	50.02	NO	27.237	NO
IND 405	1.5	120	42	Sitting	2.0744	0.01	0.15	NO	5001.443	NO
				Accident		1.40	18.79	NO	38.833	NO
UMA 90	1.4	30	30	Sitting	2.2038	0.01	0.14	NO	5154.433	NO
				Accident		1.39	17.47	NO	40.021	NO
GHBMC	0.38	0.5	3.9 Trab; 146 Cort	Sitting		0.01	0.73	NO	403.486	NO
				Accident		0.76	93.40	YES	13.703	NO

This paper is a student paper from the 19th Injury Biomechanics Symposium and is published in a special issue of SAE International Journal of Transportation Safety. It is preliminary work, has not been peer reviewed, and should not be cited because it is a work in progress.

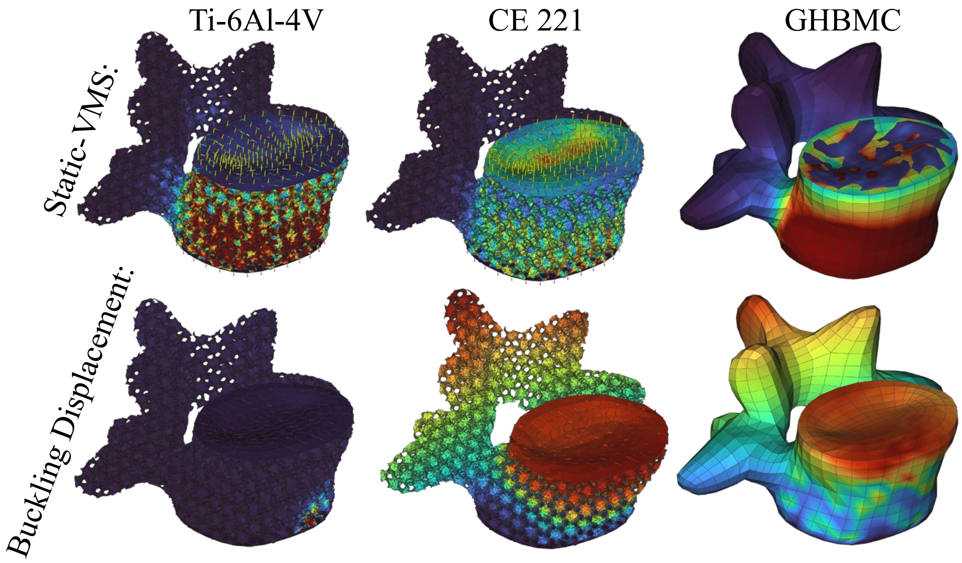

Figure 3: VMS and buckling displacement maps in L5 and GHBMC for different materials. Red = critical threshold.

Anisotropic Mimicry Results

Figure 4 presents the resulting average curves with binomial and Gaussian confidence intervals where appropriate. At an α-level of 1%, in materials with Elastic Modulus between 2.98 and 36.6 GPa, there is at least an 80% probability of constraint satisfaction.

This paper is a student paper from the 19th Injury Biomechanics Symposium and is published in a special issue of SAE International Journal of Transportation Safety. It is preliminary work, has not been peer reviewed, and should not be cited because it is a work in progress.

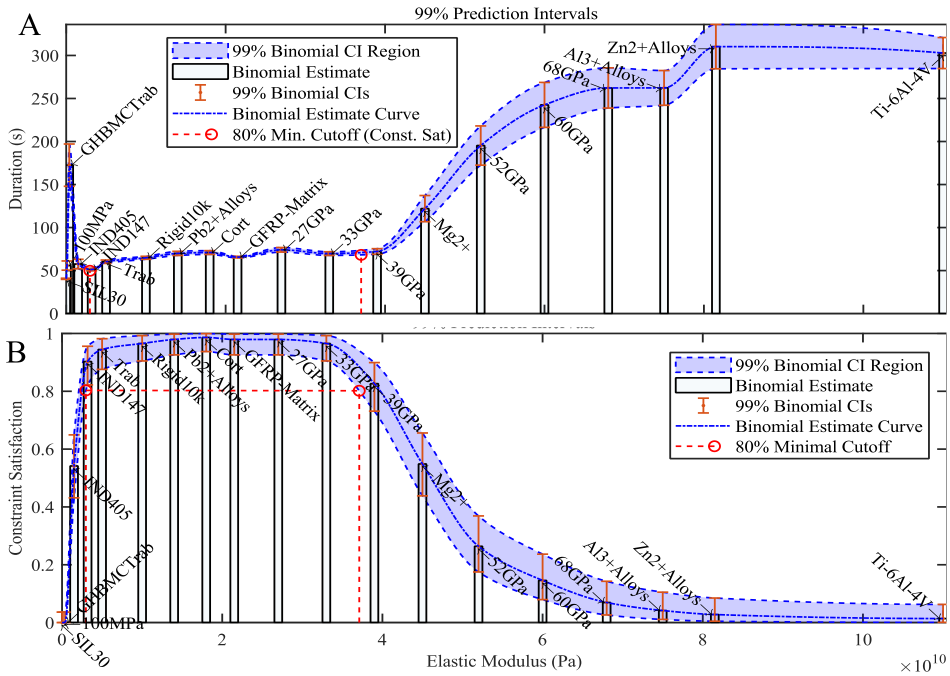

Figure 4: (A) 3D IH duration vs. E; and (B), Constraint satisfaction vs. E.

DISCUSSION

The isotropy mimicry portion of this study was limited by cell size. As cell size was reduced to allow for more complex effective structures, the number of elements needed for modeling increased dramatically. As unit cell size decreases, the number of elements increases significantly with edge length decreasing and the number of unit cells increasing. This influences mesh size drastically. Typically, practitioners of implicit design strive to create satisfactorily complex parts. The structures herein met the desired standard for complexity but could not exceed that which was desired.

Replicates are not used here since consistent results are anticipated per run, sparing numerical error as a confounding possibility. Via logistic regression, as rigidity increases, so do the odds of material failure in an accident (p=0.0095). Neither modal nor material failure are observed when sitting. Supporting the hypothesis, an optimal balance of thickness and mechanics yields analogous properties.

The valid range for IH from the Results section spans a broad range of materials that can be additively manufactured, from standard photopolymers to glass filled composites. Supporting the hypothesis, it is statistically observed that there is an optimal range of materials for microstructural mimicry, outside of which constraint satisfaction is highly improbable.

CONCLUSIONS

For isotropic mimicry of bulk skeletal constructs, it is observed that a target material exists with the ideal properties to mimic buckling and material phenomena. The closest here was Fortify DT. For pure anisotropy skeletal microstructure mimicry, it is concluded that construction-material elasticity can be used to assess probability of successful inverse homogenization. This work may lend insight into the considerations necessary when designing 3D microstructures that mimic tensorial properties present in continuum mechanics.

ACKNOWLEDGEMENTS

We would like to acknowledge support from the Wake Forest University/Virginia Tech School of Biomedical Engineering and Sciences, as well as the NASA/North Carolina Space Grant Consortium for funding time on this great research. Additionally, we would like to thank Dr. Scott Gayzik for administering the semester project in the course on Human Modeling, which comprises the work on isotropic mimicry herein.

REFERENCES

Gibson, L. J., & Ashby, M. F. (2014). Cellular solids: Structure and properties, second edition. *Cellular Solids: Structure and Properties, Second Edition*, 1–510. https://doi.org/10.1017/CBO9781139878326

Gibson, L. J., Ashby, M. F., Schajer, G. S., & Robertson, C. I. (1982). The mechanics of two-dimensional cellular materials. *Proceedings of the Royal Society of London. A. Mathematical and Physical Sciences*, *382*(1782), 25–42. https://doi.org/10.1098/RSPA.1982.0087

Hazrati-Marangalou, J., Ito, K., Cataldi, M., Taddei, F., & Van Rietbergen, B. (2013). A novel approach to estimate trabecular bone anisotropy using a database approach. *Journal of Biomechanics*, *46*(14), 2356–2362. https://doi.org/10.1016/j.jbiomech.2013.07.042

Lopes, P. C. F., Pereira, A. M. B., Clua, E. W. G., & Leiderman, R. (2022). A GPU implementation of the PCG method for large-scale image-based finite element analysis in heterogeneous periodic media. *Computer Methods in Applied Mechanics and Engineering*, *399*, 115276. https://doi.org/10.1016/J.CMA.2022.115276

National Safety Council. (2023). *Historical Car Crash Deaths and Rates - Injury Facts*. https://injuryfacts.nsc.org/motor-vehicle/historical-fatality-trends/deaths-and-rates/

Refai, K., Montemurro, M., Brugger, C., & Saintier, N. (2020). Determination of the effective elastic properties of titanium lattice structures. *Mechanics of Advanced Materials and Structures*, *27*(23), 1966–1982. https://doi.org/10.1080/15376494.2018.1536816

Scherer, M. R. J. (2013). *Double-Gyroid-Structured Functional Materials* [Springer International Publishing]. https://doi.org/10.1007/978-3-319-00354-2

Sigmund, O. (1994). Materials with prescribed constitutive parameters: An inverse homogenization problem. *International Journal of Solids and Structures*, *31*(17), 2313–2329. https://doi.org/10.1016/0020-7683(94)90154-6